Applied Surface Science xxx (2014) xxx–xxx

Contents lists available at ScienceDirect

Applied Surface Science

journal homepage: www.elsevier.com/locate/apsusc

Laser sintering of magnesia with nanoparticles of iron oxide and aluminum oxide

L.V. García [a], M.I. Mendivil [a], T.K. Das Roy [a], G.A. Castillo [a], S. Shaji [a,b,*]

[a] Facultad de Ingenieria Mecanica y Electrica, Universidad Autonoma de Nuevo Leon, Av. Pedro de Alba s/n, Cd. Universitaria, San Nicolas de los Garza, Nuevo Leon 66451, Mexico
[b] CIIDIT, Universidad Autonoma de Nuevo Leon, Apodaca, Nuevo Leon, Mexico

ARTICLE INFO

Article history:
Received 30 June 2014
Received in revised form
14 September 2014
Accepted 22 September 2014
Available online xxx

Keywords:
Laser sintering
Nanoparticles
Structure
Morphology
XRD
SEM
XPS.

ABSTRACT

Nanoparticles of iron oxide (Fe_2O_3, 20–40 nm) and aluminum oxide (Al_2O_3, 50 nm) were mixed in different concentrations (3, 5 and 7 wt%) in a magnesium oxide (MgO) matrix. The mixture pellet was irradiated with 532 nm output from a Q-switched Nd:YAG laser using different laser fluence and translation speed for sintering. The refractory samples obtained were analyzed using X-ray diffraction technique, scanning electron microscopy and X-ray photoelectron spectroscopy. The results showed that the samples irradiated at translation speed of 110 μm/s and energy fluence of 1.7 J/cm^2 with a concentration of 5 and 7 wt% of Fe_2O_3 presented the $MgFe_2O_4$ spinel-type phase. With the addition of Al_2O_3 nanoparticles, at a translation speed of 110 μm/s and energy fluence of 1.7 J/cm^2, there were the formations of $MgAl_2O_4$ spinel phase. The changes in morphologies and microstructure due to laser irradiation were analyzed.

1. Introduction

Sintering of ceramic compounds is usually implemented with a convection oven sintering, therefore a long sintering time and high thermal load. Some alternative methods for sintering are chemical densification [1], electrical [2], pressure, laser [3–5] and microwave sintering [6,7]. The melting temperature of the metal NPs can be reduced to the range of 100–200 °C due to their thermodynamic size effect [8,9]. This novel property of metal NPs resulted in low-temperature thermal sintering process taking advantage of the reduced melting temperature, reduced heat conductivity and field enhancement between the NPs. This process was successfully applied for the fabrication of high-performance OFETs (organic field-effect transistor) due to the combination of the ultra-short pulse of the femtosecond laser and the novel thermal characteristics of the metal NPs. Seung Hwan Ko et al. [10] reported a high-resolution metal nanoscale digital patterning with direct femtosecond laser sintering of solution-deposited metal NPs.

The laser beam is usually in accordance with the Gaussian distribution, and the beam power is the greatest at the centre of the beam. Hence, the beam affects only a small area at a time. A laser beam also has limited depth that it can affect directly. Pulsed lasers produce short pulse duration with great intensity and have better penetration of the material than continuous wave lasers. In addition, the wavelength and absorption have an effect on penetration depth. Laser sintering is dependent on the incident power, the absorption to the material and the interaction time [11]. Laser sintering is a selective sintering method, which makes it possible to process selectively local areas within the material. Laser annealing was used in the performance of different structures where a highly local heating/melting of one of their components at nano-micro-scale was necessary, as the laser annealed TiO_2 electrodes for dye-sensitized solar cells [12]. Minyang Yang et al. [13] reported a laser direct patterning method for the fabrication of flexible electronics on heat-sensitive polymer substrates. Air-stable OFETs fabricated by selective laser sintering of inkjet printed metal nanoparticles, in which the local thermal control helped to avoid thermal damage to the substrate [14] was known.

Grigoropoulos and co-workers studied low-temperature sintering using metal nanoparticles inks [15] and also reported the fabrication of highly conductive transparent ZnO films by ultra-short pulsed laser annealing [16]. The study was developed examining the variations of the conductivity and transmittance of the ZnO thin films by altering the annealing parameters such

* Corresponding author.
E-mail addresses: sshajis@yahoo.com, sadasivan.shaji@uanl.edu.mx (S. Shaji).

http://dx.doi.org/10.1016/j.apsusc.2014.09.140
0169-4332/

as laser power, translation speed and background gas. Thin-film transistor was fabricated by excimer laser annealing of ZnO nanoparticles [17]. In another work [18], they reported the optical near-field nanoprocessing of nanoparticles for high-throughput nanomanufacturing using assembled microspheres as a near-field optical confinement structure array for laser-assisted nanosintering and nanoablation of nanoparticles taking advantage of the low processing temperature and reduced thermal diffusion in the nanoparticle film. Hwang Ko et al. [19,20] studied the direct metal patterning on flexible polymer substrates by applying CW laser on solution deposited Ag NP ink film. Barcikowski et al. [21] took advantage of the laser sintering efficiency for the fabrication of hybrid compounds with a smooth and homogeneous surface, in particular, for additive manufacturing. Simulation studies of nanoscale sintering were reported due the emerging of new mechanisms at this scale where the neck growth between Au nanoparticles was analyzed by low-energy laser irradiation [22]. In this work, we analyzed the effects of the laser energy fluence, translation speed and oxide nanoparticle concentrations (Fe_2O_3 andAl_2O_3) in samples of the ceramics matrix (MgO). Variation of these parameters showed that the sintering process was affected with these changes.

2. Experimental

2.1. Preparation of MgO matrix with nanoparticles

Calcined magnesia (MgO) with a particle size <45 μm was taken as raw material. The MgO powder was sieved by a mesh 320. High-purity nano-iron oxide (α-Fe_2O_3) and alumina oxide (α-Al_2O_3) with an average particle size in the range of 20–50 nm (Skyspring Nanomaterials, Inc., USA) was used. For α-Fe_2O_3 and α-Al_2O_3 nanoparticles, the concentrations used were 3, 5 and 7 wt%. In order to obtain a suitable and stable suspension of nano-oxides, a dispersion process was carried out using a dispersant (Zephrym) and acetone as a dispersion medium and then applying an ultrasonic agitation during 30 min. The powders were mechanically homogenized during 10 min, then uniaxial pressed into a metallic mold to obtain cylindrical samples (0.4 cm height × 1.0 cm diameter) using a pressure of 100 MPa. Refractory pellets were made based on the nano-Fe_2O_3 + MgO and nano-Al_2O_3 + MgO combination of materials.

2.2. Laser sintering

After pressing, compacted refractory pellets were irradiated with a pulsed Nd:YAG laser. The experiments were performed using the second harmonic (532 nm) of a Nd:YAG laser (Solar Laser System, LQ 929) operated at 10 Hz with a pulse width of 10 ns. The output laser beam was focused with a convex lens (with a focal length 200 mm) over the pellets surfaces. The working distance was varied adjusting the distance between the convex lens and the pellets surface at 115 and 125 mm. Laser energy fluence of 0.8 and 1.7 J/cm^2 were calculated at respective working distances. The pellets were mounted in a linear translation device with three different translation speeds of 550, 400 and 110 μm/s. All the pellets were irradiated two times in two different directions. The main focus was to study the effects of concentration of nanoparticles (Fe_2O_3 and Al_2O_3), energy fluence and the translation speed on the structure and morphologies of laser sintered refractory matrix.

2.3. Characterization

The crystalline structure, morphology and composition of the laser-irradiated pellets were characterized by X-ray diffraction (XRD), scanning electron microscopy (SEM), energy-dispersive X-ray spectroscopy (EDX in SEM) and X-ray photoelectron spectroscopy (XPS) techniques. The X-ray diffraction patterns were recorded by Bruker D8 Advance diffractometer using Cu Kα_1 radiation (λ = 1.54056 Å). The scan range (2θ) was from 10° to 90° at a scan speed of 1°/s. The surface morphologies of as-prepared and laser-sintered refractory pellets were examined by scanning electron microscope (FEI Nova NanoSEM200). X-ray photoelectron spectroscopy (XPS) study was done using a Thermo Scientific K-alpha X-ray photoelectron spectrometer system. The samples were excited by a monochromatized Al Kα X-ray radiation of energy 1486.6 eV. All the spectra reported in this paper were recorded with reference to C 1s peak (284.6 eV).

3. Results and discussion

3.1. Structural analysis

Structural characterization of the pellets formed at different nano-oxide concentrations irradiated with different laser energy fluence and translation speeds was obtained from their XRD patterns. Fig. 1 shows the diffraction patterns of the pellets of MgO/Fe_2O_3 laser irradiated with the translation speed of 110 μm/s. The concentration of Fe_2O_3 NPs was 7 wt%. Fig. 1a and b shows the pellets (7% nano-Fe_2O_3–MgO) with different energy fluence of 1.7 and 0.8 J/cm^2 respectively. Fig. 1c and d shows the XRD pattern of pellets irradiated using fluence of 1.7 J/cm^2 having the concentration of NPs as 5 and 3 wt%, respectively. The planes diffracted at (1 1 1), (2 0 0), (2 2 0), (3 1 1) and (2 2 2) were identified and indexed comparing with the standard pattern PDF # 0045-0946 corresponding to MgO matrix. In the same way, the planes (1 1 1), (3 1 1), (4 2 2) and (5 3 3) were matched with the standard pattern of $MgFe_2O_4$ (PDF # 0014-7519). As an effect of the concentration of Fe_2O_3 nanoparticles, an increment of peak intensities corresponding to $MgFe_2O_4$ crystalline phase was observed. Higher concentration of nanoparticles resulted with increased formation of the spinel. Also, better intensities for the MgO peaks were observed for higher concentrations of nanoparticles due to improved sintering effect. Some 2θ degree values which were correspondent to planes (2 2 2), (4 0 0), (4 4 0), (5 3 3) and (4 4 4) were shared between MgO and $MgFe_2O_4$.

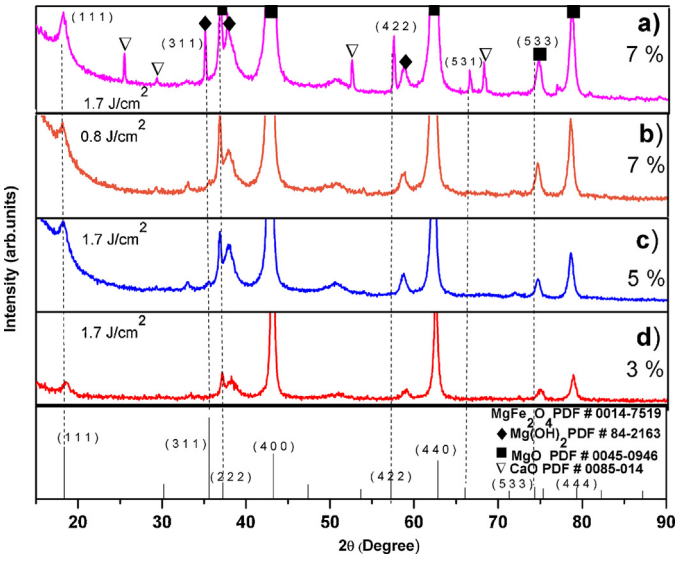

Fig. 1. XRD patterns of MgO/Fe_2O_3 refractory pellets irradiated by the 532 nm output of a Nd:YAG laser system and translation speed of 110 μm/s. (a, b) 7 wt% of iron oxide nanoparticles that were irradiated at energy fluence of (a) 1.7 J/cm^2 and (b) 0.8 J/cm^2. The XRD pattern for (c) 5 wt% and (d) 3 wt% of Fe_2O_3 nanoparticles irradiated at 1.7 J/cm^2 of energy fluence with the standard JCPDS data for $MgFe_2O_4$ (PDF # 0014-7519).

Please cite this article in press as: L.V. García, et al., Laser sintering of magnesia with nanoparticles of iron oxide and aluminum oxide, Appl. Surf. Sci. (2014), http://dx.doi.org/10.1016/j.apsusc.2014.09.140